АСТРОФИЗИКА

ТОМ 48 ФЕВРАЛЬ, 2005 ВЫПУСК 1

УДК: 524.7

IRAS F02044+0957: AN INTERACTING SYSTEM

V.H.CHAVUSHYAN[1,2], O.V.VERKHODANOV[3,4], J.R.VALDÉS[1], R.MÚJICA[1], S.A.TRUSHKIN[3]

Received 1 September 2004
Accepted 10 November 2004

A list of 750 objects has been compiled using the Astrophysical CATalogs Support System (CATS) database, by cross-identifying sources in the IRAS catalogues and the catalogue of Texas survey at 365 MHz. We have carried out a search for optical counterparts of those objects, where the difference in positions between the two catalogues and the APM is less than 3". One of these sources, IRAS F02044+0957, was observed with the RATAN-600 radio telescope at four frequencies in April 1999. Optical spectroscopy of the components of the system was made with the 2.1-m telescope of the Guillermo Haro Observatory. The radio and optical spectra, the NVSS radio map and the optical and infrared images allow us to conclude that the steep spectrum ($\alpha = -0.94 \pm 0.02$) radio source IRAS F02044+0957 is a pair of interacting galaxies, a LINER and a HII galaxy, at $z = 0.093$.

Keywords: *Galaxies: interactions - Infrared: galaxies - Radio continuum: galaxies*

1. *Introduction.* Using the CATalogs Support System database (CATS, [1]) to cross-identify sources in the IRAS and Texas Survey [2] at 365 MHz catalogues, Trushkin and Verkhodanov [3,4] have compiled a list of about 750 objects. These objects have been classified on the basis of their radio spectrum, and two samples, one of steep spectrum radio sources ($S \sim \nu^{\alpha}$), with $\alpha < -0.9$ (128 objects), and the second of inverted spectrum, with $\alpha > 0.0$ (28 objects), were selected for further study. We searched for optical counterparts of the most reliable candidates, for which the IRAS, Texas Survey and optical positions agreed within 3" [5]. Optical positions were taken from the Automatic Plate Measuring machine (APM) catalogue of the Palomar Observatory Sky Survey (POSS). From the sample of steep spectrum sources, we selected those without classifications in public databases; CATS, NASA/IPAC Extragalactic database (NED), and Lyon-Meudon Extragalactic database (LEDA). One of these objects is IRAS F02044+0957, identified with the NRAO VLA Sky Survey (NVSS) [6] radio source J020706+101147.

Since the spatial resolution of the IRAS survey at 60 μm is about 1.5'/pix, no additional details could be found in the corresponding infrared image of IRAS F02044+0957. The flux density at 60 μm is 0.63 Jy, while at 12, 25, and 100 μm only upper limits are reported in the IRAS Faint Source catalogue (see Table 1). The 20'x20' DSS1 E-plate image of IRAS F02044+0957, with the NVSS radio isophotes superposed is shown in Fig.1. Two extended objects

were found at the position of the IRAS source. The inspection of the higher spatial resolution DSS2 E-plate image shows that each of these extended objects was a double system (A-B and C-D, see Fig.2 and Table 2 for more

Table 1

OBSERVATIONAL PARAMETERS AND IR FLUXES OF IRAS F02044+0957

Catalogue name	IFSC F02044+0957
RA, DEC (J2000)	020706.0 + 101148.1
$\Delta_{RA} \times \Delta_{Dec}$	$1.2^s \times 9''$
S 12 μm, Jy	0.38
S 25 μm, Jy	0.33
S 60 μm, Jy	0.67
S 100 μm, Jy	1.00

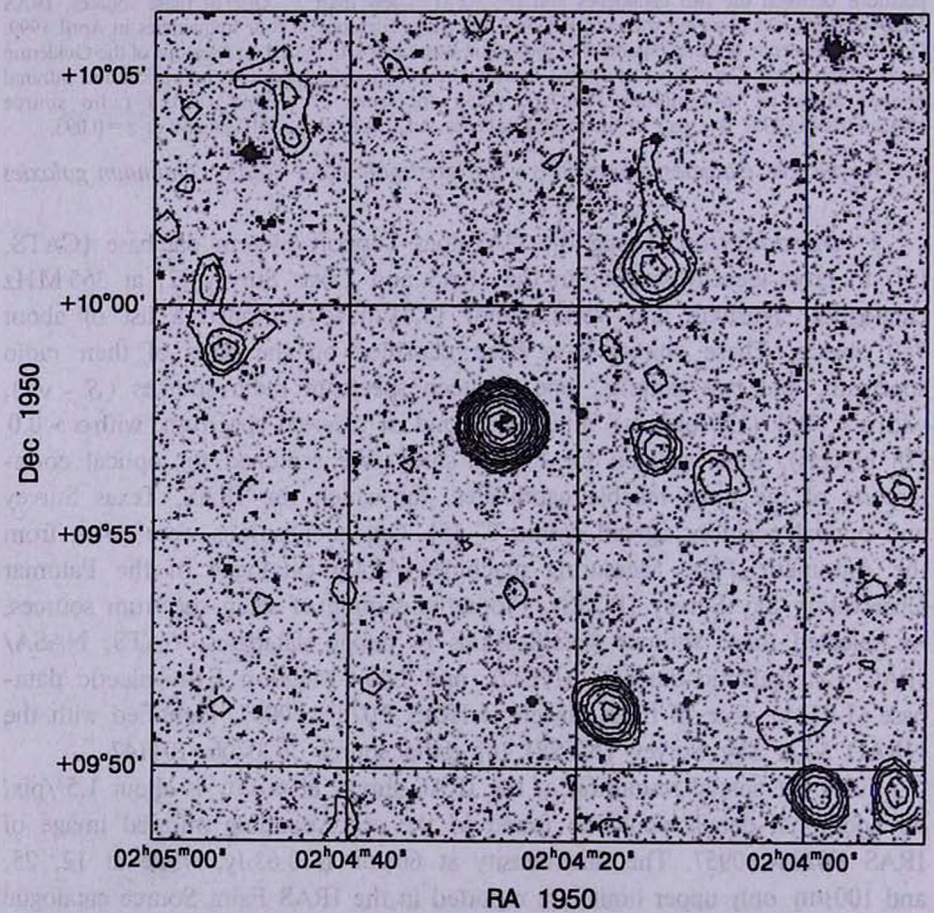

Fig.1. The NVSS radio isophotes overlaid on the DSS1 20' x20' image centered on IRAS F02044+0957. The radio isophotes are plotted in a linear scale with a step of 0.8 mJy/beam from the level of 0.8 mJy/beam. The rms of the map is 0.45 mJy/beam.

details). Therefore, taking into account the complexity of IRAS F02044+0957, we decided to study it, in order to determine the probable interacting nature of its components.

Table 2

THE COORDINATES AND MAGNITUDES OF THE IRAS F02044+0957 COMPONENTS FROM THE US NAVAL OBSERVATORY (USNO) CATALOGUE

Component	R.A. J2000.0	Dec. J2000.0	Blue magnitude
A	02 07 06.09	+10 11 47.4	16.0
B	02 07 06.24	+10 11 46.7	16.7
C	02 07 06.38	+10 11 33.5	...
D	02 07 06.67	+10 11 37.8	14.6[1]
E[2]	02 07 08.50	+10 11 17.9	19.1

[1] The magnitude of the C + D components.
[2] This object fell on the slit (see the discussion).

Here we report the results of the analysis of the radio properties of IRAS F02044+0957 system and of the spectroscopy study of its components. In

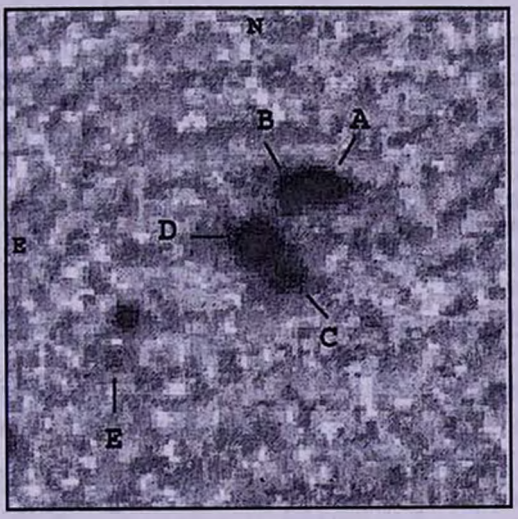

Fig.2. The 1'.5 x 1'.5 DSS2 image of IRAS F02044+0957. The source was resolved into four components (A, B, C, and D).

Sec.2 we describe the radio and optical observations. In sec.3 we discuss the results, and the conclusions are presented in Sec.4.

2. *Observation.*

2.1. *RATAN-600 observations.* Radio observations were carried out in

April 23-25, 1999 with the North Sector of the RATAN-600 telescope. The wide-band radiometer complex at four frequencies: 2.3, 3.9, 7.7 and 11.2 GHz, was used. The nearby non-variable radio source PKS 1345+12 was used as the flux density calibration source. The RATAN-600 radio flux densities, and those taken from the Texas and NVSS catalogues are given in Table 3.

The Texas radio interferometer and NVSS beam sizes were about 54" and 45", respectively. IRAS F02044+0957 is described as a pointlike source in [2] and [6]. However, Condon et al. [6] give an upper limit for the NVSS size of this object of 17".4 x 17".0.

2.2. *Optical observations and data reduction.* Optical spectroscopy of objects, marked A, B, C, D, and E in Fig.2, was obtained in August and November 1999. We used the 2.1-m telescope of the Guillermo Haro Observatory (GHO) in Cananea, Sonora, México, operated by the National Institute of Astrophysics, Optics and Electronics (INAOE). The Landessternwarte Faint Object Spectrograph and Camera (LFOSC, [7]) was used. A setup covering the spectral range λ4200 - 9000 Å with a dispersion of 8.2 Å/pix was adopted. The effective instrumental spectral resolution is about 15 Å.

Table 3

THE RADIO FLUXES OF IRAS F02044+0957

ν MHz	S mJy	ΔS mJy	Survey/Telescope
365	398	51	TXS
1400	76.3	2.3	NVSS
2300	60	10	RATAN
3900	45	10	RATAN
7700	21	7	RATAN
11200	15	4	RATAN

Data reduction was done using the IRAF[1] packages and included bias and flat field corrections, cosmic rays cleaning, wavelength linearization and flux calibration. Fig.4 shows the optical spectra of objects A, B, C, and E. Object D is a star, its spectrum is shown in Fig.5.

The integrated emission line fluxes were determined by means of the spectral analysis software package, developed by Vlasyuk (private communication) at the Special Astrophysical Observatory. With this software is possible to determine the best-fit Gaussian profile of emission lines, and to deblend closely spaced lines, as is the case of Hα λ6563 Å and [NII]

[1] *IRAF is the Image Reduction and Analysis Facility distributed by the National Optical Astronomy Observatories, which is operated by the Association of Universities for Research in Astronomy (AURA) under agreement with the National Science Foundation (NSF).*

λλ 6548, 6584 Å lines. In our data, this blending is due to the combined effects of the spectral resolution of the spectrograph and to the intrinsic width of the emission lines of the objects. In order to measure the intensities of Hα + [NII] components we have used a three Gaussian component function

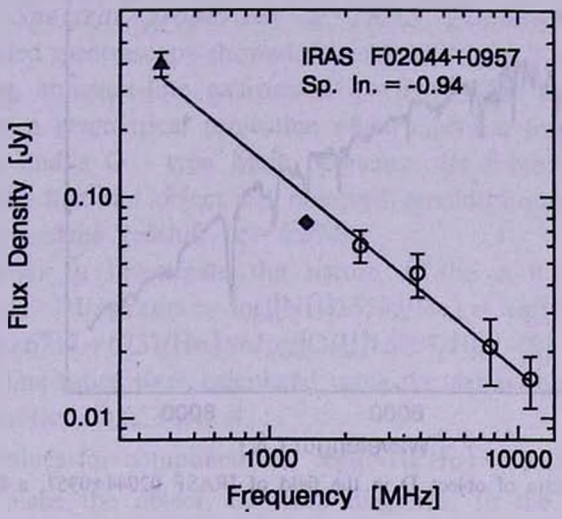

Fig.3. The radio spectrum of IRAS F02044+0957. Open circles represent the RATAN measurements.

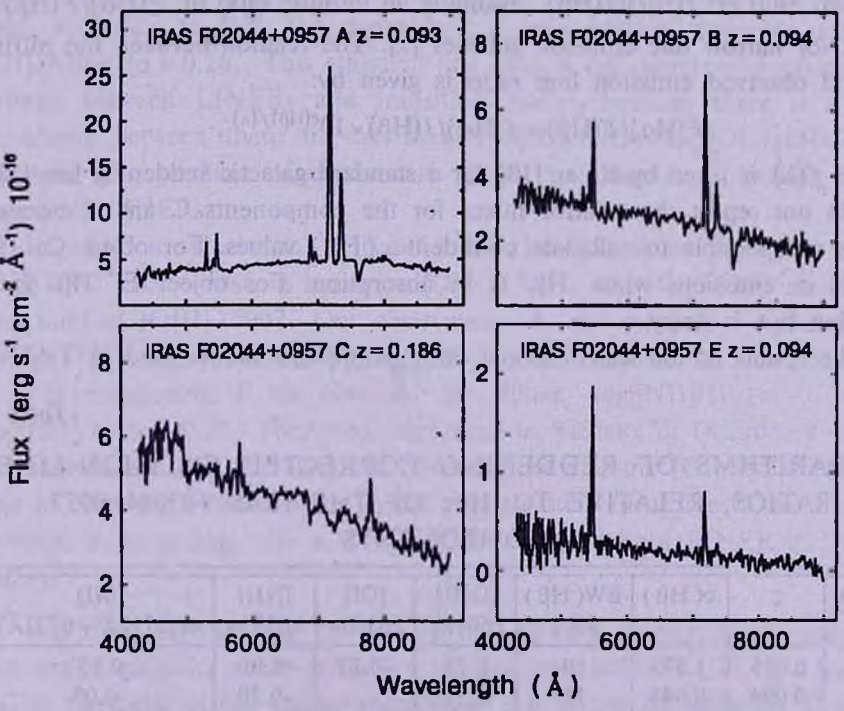

Fig.4. The optical spectra of objects A, B, C, and E in the IRAS F02044+0957 field. Telluric bands at λ6867Å, λ7186Å and λ7594Å were not substracted.

with a fixed theoretical value of [NII]λ6583/[NII]λ6548 = 3.0 [8] and assuming the same *FWHM* for both lines.

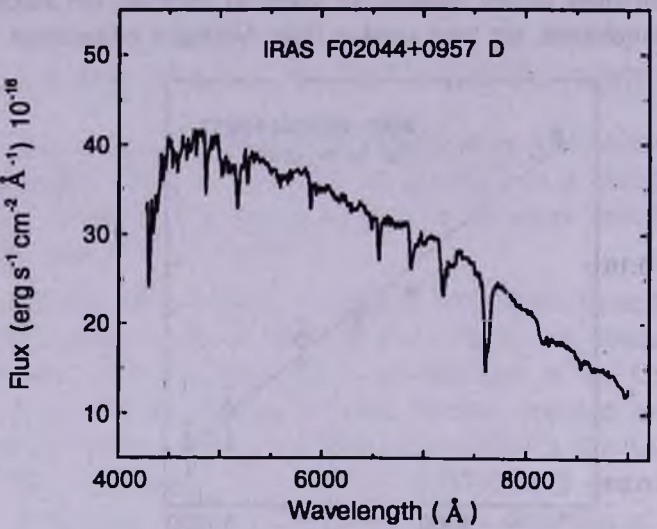

Fig.5. The optical spectra of object D in the field of IRASF 02044+0957, a G-type star.

The value of the dust reddening coefficient $c(\mathrm{H}\beta)$ was determined from the observed ratio of $I(\mathrm{H}\alpha)/I(\mathrm{H}\beta)$, assuming an intrinsic ratio of $F(\mathrm{H}\alpha)/F(\mathrm{H}\beta) = 2.85$ for narrow line emission galaxies [9]. The relation between the intrinsic and observed emission line ratio is given by:

$$F(\mathrm{H}\alpha)/F(\mathrm{H}\beta) = I(\mathrm{H}\alpha)/I(\mathrm{H}\beta) \times 10^{c(\mathrm{H}\beta)f(\lambda)},$$

where $f(\lambda)$ is listed by Kaler [10] for a standard galactic reddening law [11]. We do not report the relative fluxes for the components C and E because it was not possible to calculate confident $c(\mathrm{H}\beta)$ values. For object C, Hα line is in emission, while Hβ is in absorption. For object E, Hβ is in emission but is noisy.

The results of the spectroscopic observations are summarized in Table 4.

Table 4

LOGARITHMS OF REDDENING CORRECTED EMISSION-LINE RATIOS, RELATIVE TO Hβ, OF THE IRAS F02044+0957 COMPONENTS

Comp.	z	c(Hβ)	EW(Hβ) (Å)	[OIII] λ5007Å	[OI] λ6300Å	[NII] λ6583Å	[SII] λλ(6717Å + 6731Å)
A	0.093	1.377	19	0.26	-0.13	0.30	0.23
B	0.094	0.645	11	0.31	...	-0.30	-0.09
C	0.186	...	...	...	...	...	...
E	0.094	...	...	...	...	...	...

The reddening corrected intensities are normalized to Hβ flux. The uncertainty in the intensity ratios is less than 30%, for all emission lines reported here. It corresponds to an uncertainty of about 0.1 in the logarithm of the intensity ratios.

3. *Discussion.*

3.1. *Spectral properties of IRAS F02044+0957 components.*

The detailed spectroscopy showed that objects A and B are apparently a pair of interacting emission-line galaxies at $z = 0.093$. The second pair, objects C and D, is a geometrical projection of an emission line galaxy (object C) at $z = 0.186$, and a G - type Main Sequence star (object D). It is noteworthy to mention that the object E, observed serendipitously with objects A and B, has the same redshift ($z = 0.094$).

In order to investigate the nature of the A-B system, we used the diagnostic diagrams $\log([\text{NII}]\lambda 6583/\text{H}\alpha)$ vs $\log([\text{OIII}]\lambda 5007/\text{H}\beta)$ and $\log([\text{SII}]\lambda\lambda 6717+6731/\text{H}\alpha)$ vs $\log([\text{OIII}]\lambda 5007/\text{H}\beta)$ [9]. The corresponding emission-line ratios were calculated using the extinction corrected, relative to Hβ intensities from Table 4.

The values for component A, $\log([\text{NII}]/\text{H}\alpha) = -0.15$ and $\log([\text{SII}]/\text{H}\alpha) = -0.23$, place the object, on both diagrams, in the AGN region, but in a position very close to the boundary with the HII-like galaxies. In order to solve this uncertainty, we used a second criterion for spectral classification, according to [12], the component A is a LINER since the value of $[\text{OI}]\lambda 6300/\text{H}\alpha = 0.26$. This emission-line ratio is the principal discriminating criteria between LINERs and transition nuclei, because there is a clear separation between them in the $\log([\text{OI}]\lambda 6300/\text{H}\alpha)$ vs $\log([\text{OIII}]\lambda 5007/\text{H}\beta)$ diagram. The position of component A in this diagram is located in the region of LINERs.

In addition, Heckman [13] defined a LINER as an object in which [OII] λ3727 is, at least, as strong as [OIII] λ5007, and [OI] λ6300 is, at least, one third of [OIII] λ5007. Our observations do not cover the region around [OII] λ3727, but [OI]λ6300/[OIII]λ5007 is equal to 0.40 for component A.

For component B we obtained the values: $\log([\text{NII}]/\text{H}\alpha) = -0.76$ and $\log([\text{SII}]/\text{H}\alpha) = -0.55$. Therefore, according to Veilleux & Osterbrock criteria [9], component B is an HII galaxy. We can not measure [OI] λ6300 emission line in this object, because the line is strongly affected by the O_2 atmospheric B-band. Summarizing, the A-B system is composed by a LINER and a HII galaxy.

3.2. *The interacting nature of the system.*

A significant fraction of the active galactic nuclei (AGNs) are infrared emitters [14,15]. In such AGNs the peak of the energy distribution lies in the far infrared. This fact,

together with radio emission, are important signs of central activity. We estimate the infrared luminosity for IRAS F02044+0957, at 60 μm, $L_{60\mu m} = 4 \times 10^{38}$ erg sec^{-1} cm^{-2}, which is larger than the radio luminosity (see below) and the optical luminosity, $L_{Opt} = 2.4 \times 10^{37}$ erg sec^{-1} cm^{-2}, calculated from the USNO Blue magnitude (the flux density is 0.87 mJy for a 16.7 mag, see identification in Table 2). Thus, both properties mentioned above have been found in the IRAS F02044+0957 source.

The realibility of radio and infrared identifications was estimated by the Likelihood ratio [16], determined from

$$LR(r) = [1/(2\lambda)]\exp\left[0.5 \times r^2(2\lambda - 1)\right]$$

where $\lambda = \pi \times \sigma_{RA} \times \sigma_{Dec} \times \rho$; ρ is the density of the background sources, we assumed that $\rho = 5.16 \times 10^{-4}$ objects per arcsec^2 for high galactic latitudes [17]; $r = \left[(\Delta RA/\sigma_{RA})^2 + (\Delta Dec/\sigma_{Dec})^2\right]^{1/2}$, ΔRA and ΔDec are the differences of the radio and optical positions of the object; σ^2_{RA} and σ^2_{Dec} are correspondingly, $\sigma^2_{radio} + \sigma^2_{optical}$. The identification is considered as reliable if LR > 2.

The corresponding likelihood ratios were calculated and are listed in Table 5. Both components have LR > 2 for the radio counterpart, and close to 2 for the infrared counterpart. However, based on the values of Table 5, component B is the most probable source of radio and infrared emission.

Table 5

LIKELIHOOD RATIOS FOR RADIO AND INFRARED IDENTIFICATIONS OF THE IRAS F02044+0957 COMPONENTS

Comp.	LR_{RADIO}	LR_{IR}
A	28.70	1.52
B	73.90	1.56
C	0.00	0.95
D	0.00	1.27

The radio emission from the A-B system has a steep non-thermal spectrum. The spectral index, $\alpha = -0.94 + 0.02$, was estimated from a linear least squares fit to the radio spectrum. Each point of the spectrum was weighted proportionally to the inverse square of the relative error of the flux density $1/(\Delta S/S\nu)^2$. The radio spectrum of IRAS F02044+0957 is described by a power-law $S\nu$ [Jy]=85×$\nu^{-0.94\pm0.02}$ MHz, and is shown in Fig.3. The spectral index for IRAS F02044+0957, obtained by only combining the 365 KHz (Texas survey) and 1.4 GHz (NVSS) fluxes, is $\alpha = -1.23$, which is not in agreement with our estimation. The radio luminosity, in the frequency interval from 365 to 10^4 MHz, is $L_R = 9.4 \times 10^{34}$ erg sec^{-1} cm^{-2} (assuming $H_0 = 70$ km sec^{-1} Mpc^{-1}, and $q_0 = 0$).

The infrared emission of this system, according to the standard hypothesis, can be due to dust produced as a result of enhanced star formation [18], which is triggered by the interaction of galaxies. However, it is not yet clear what mechanism powers the bolometric luminosity of Luminous Infrared Galaxies (LIRGs). Perhaps the tightest constraint on the nature of the infrared luminosity is the FIR/Radio correlation that normal star forming galaxies mostly obey [19]. Nevertheless, we can not rule out the contribution to the luminosity coming from an AGN component.

LIRGs are often found in interacting systems, indicating the two phenomena may be triggered at once by dynamical interactions [20]. The interacting nature of IRAS F02044+0957 is confirmed from the redshift distribution of the system's components, obtained from our optical spectroscopy.

In order to clarify the nature of the infrared emission of IRAS F02044+0957 we investigated the FIR-Radio correlation for this system. In star-forming galaxies, FIR and radio emissions are tightly correlated over a wide range of IR luminosities [19]:

$$q = \log\{[F_{FIR}/(3.75\times10^{12}\,\mathrm{Hz})]/[f_\nu(1.49\,\mathrm{GHz})]\} = 2.35\pm0.2\,.$$

For IRAS F02044+0957 the parameter $q = 1.08$. There are some possibilities to explain this discrepancy. Panuzzo et al. [21] have shown that in normal star-forming galaxies deviations from this relation are due to variations of the corresponding FIR luminosity as the latter depends more on the details of the obscuration. In starburst galaxies, if the starburst is in a late phase and the star formation decreased exponentially, there is an excess of radio emission [22].

Condon et al. [23] concluded that most LIRGs in the Bright Galaxy Sample (BGS) can be modeled by a ultraluminous nuclear starburst. These starburst regions would be so dense and would be optically thick even to free-free absorption at 1.49 GHz, and to dust absorption for $\lambda < 25\,\mu\mathrm{m}$.

The spectral energy distribution, from infrared to radio wavelengths, of IRAS F02044+0957 is typical for low luminosity normal galaxies (see Fig.2 in [19]). Various models of the infrared emission [24,25] have suggested that in this kind of galaxies the secondary peak in the mid-infrared is due to emission from small dust grains near hot stars, while the stronger peak at $\lambda > 100-200\,\mu\mathrm{m}$ represents emission dominated by dust from infrared cirrus heated by the older stellar population.

Thus, we can confirm our hypothesis that the infrared emission from IRAS F02044+0957 is due to star formation induced by the interaction in the A-B system. With a high probability we are dealing with star formation processes, deeply embedded in the dust structure of this source.

4. *Conclusions*. We have carried out detailed optical spectroscopy for

the different components of IRAS F02044+0957 and studied its FIR and radio emission properties in order to determine the nature of the system.

From optical spectroscopy, we found the A-B system is a pair of interacting galaxies at $z=0.093$, composed by a LINER (component A) and a HII galaxy (component B). The C-D system is a geometrical projection of an emission line galaxy at $z=0.186$ (object C), and a G-type Main Sequence star (object D).

We can rule out the G-type Main Sequence star as the source of IR and radio emissions. From the "Likelihood ratio", the IR and radio emissions are coming, most likely, from the interacting galaxy pair (objects A and B).

We conclude that the IR emission from IRAS F02044+0957 is produced by star formation processes deeply embedded in the dust structure of the source. The star formation is probably induced by the interaction. The interacting nature of A-B system is confirmed by our optical spectroscopy. The small value of parameter $q=1.08$ is interpreted as a consequence of the dust, since in normal star-forming galaxies the deviations from the FIR-Radio relation are due to variations of the corresponding FIR luminosity as it depends more on the details of the obscuration.

The spectral energy distribution of IRAS F02044+0957, from infrared to radio wavelengths, help us to confirm our hypothesis that its infrared emission is due to star formation induced by the interaction in the A-B system. With a high probability we are dealing with star formation processes, deeply embedded in the dust structure of this source.

Acknowledgments. This research has made use of the following databases: the Digitized Sky Surveys (DSS), produced at the Space Telescope Science Institute; the NASA/IPAC Extragalactic Database (NED), operated by the Jet Propulsion Laboratory, California Institute of Technology, under contract with the National Aeronautics and Space Administration; the NASA's Astrophysics Data System Abstract Service (ADS) and the LEDA database (http://leda.univ-lyon1.fr), CATS Database - Astrophysical CATalogs support System (http://cats.sao.ru/). OVV thanks INAOE's staff for their hospitality during his visit. We would like to thank the GHO staff for its support during the observations. This work was partially supported by CONACyT research grants 39560-F. Finally, we wish to thank to Daniel Kunth for careful reading of this paper and useful remarks that helped to improve this final version.

[1] Instituto Nacional de Astrofisica, Óptica y Electronica, México, e-mail: vahram@inaoep.mx
[2] Instituto de Astronomia, UNAM, Mexico
[3] Special Astrophysical Observatory RAS, Russia
[4] Visiting Astronomer, Instituto Nacional de Astrofisica, Óptica y Electronica, México

IRAS F02044+0957: ВЗАИМОДЕЙСТВУЮЩАЯ СИСТЕМА

В.О.ЧАВУШЯН[1,2], О.В.ВЕРХОДАНОВ[3,4], Дж.Р.ВАЛДЕС[1], Р.МУХИКА[1], С.А.ТРУШКИН[3]

На основании данных каталогов CATS, посредством Кросс-корреляции источников в каталогах IRAS и Техас-обзоров на 365 MHz, составлен список 750 объектов. Проведен поиск оптических отождествлений этих объектов при условии, что различие между координатами двух каталогов и APM было меньше 3". Один из этих источников, IRAS F02044+0957, наблюдался на радиотелескопе РАТАН-600 в апреле 1999г. на четырех частотах. Оптическая спектроскопия компонентов системы проводилась с помощью телескопа 2.1-м обсерватории Г.Аро. Радио и оптические спектры, NVSS радиокарта, оптические и инфракрасные изображения позволяют заключить, что радиоисточник IRAS F02044+0957, имеющий крутой спектр ($\alpha = -0.94 \pm 0.02$), является парой взаимодействующих галактик (LINER и HII-галактика) с $z = 0.093$.

REFERENCES

1. *O.V.Verkhodanov, S.A.Trushkin, H.Andernach*, V.N.Chernenkov, In: "Astronomical Data Analysis Software and Systems VI", Eds. G.Hunt, H.E.Payne, ASP Conference Series, **125**, 322, 1997.
2. *J.N.Douglas, F.N.Bash, F.A.Bozyan et al.*, Astron. J., **111**, 1945, 1996.
3. *S.A.Trushkin, O.V.Verkhodanov*, Bulletin of SAO, **39**, 150, 1995.
4. *S.A.Trushkin, O.V.Verkhodanov*, Baltic Astronomy, **6**, 345, 1997.
5. *O.V.Verkhodanov, V.H.Chavushyan, R.Mújica, S.A.Trushkin, J.R.Valdés*, Astronomy Reports, **47**, 119, 2003.
6. *J.J.Condon, W.D.Cotton, E.W.Greisen et al.*, Astron. J., **115**, 1693, 1998.
7. *F.J.Zickgraf, I.Thiering, J.Krautter et al.*, Astron. Astrophys. Suppl. Ser., **123**, 103, 1997.
8. *D.Osterbrock*, Astrophysics of gaseous nebulae. Freeman and Company, San Francisco, 1974.
9. *S.Veilleux, D.E.Osterbrock*, Astrophys. J. Suppl. Ser., **63**, 295, 1987.
10. *J.B.Kaler*, Astrophys. J., **31**, 517, 1976.
11. *A.E.Whitford*, Astron. J., **63**, 201, 1958.
12. *L.C.Ho, A.V.Filippenko, W.L.W.Sargent*, Astrophys. J. Suppl. Ser., **112**, 315, 1997.
13. *T.M.Heckman*, Astron. Astrophys., **87**, 152, 1980.
14. *W.C.Keel, M.H.K. de Grijp*, G.K.Miley, Astron. Astrophys., **203**, 250, 1988.

15. *G.N.Rieke, M.J.Lebofsky*, ARA&A, **17**, 447, 1979.
16. *H.R. de Ruiter, H.C.Arp, A.G.Willis*, Astron. Astrophys. Suppl. Ser., **28**, 211, 1977.
17. *A.M.Cohen, R.W.Porcas, I.W.Browne et al.*, Mon. Notic. Roy. Astr. Soc., **84**, 1, 1977.
18. *D.B.Sanders, B.T.Soifer, J.H.Elias et al.*, Astrophys. J., **325**, 74, 1988.
19. *D.B.Sanders*, I.F.Mirabel, ARA&A, **34**, 749, 1996.
20. *D.Rigopoulou, H.W.W.Spoon, R.Genzel et al.*, Astron. J., **118**, 2625, 1999.
21. *P.Panuzzo, A.Bressan, G.L.Granato, L.Silva, L.Danese*, Astron. Astrophys., **409**, 99, 2003.
22. *A.Bressan, L.Silva, G.L.Granato*, Astron. Astrophys., **392**, 377, 2002.
23. *J.J.Condon, Z.-P.Huang, Q.F.Yin, T.X.Thuan*, Astrophys. J., **378**, 65, 1991.
24. *G.Helou*, Astrophys. J., **311**, 33, 1986.
25. *M.Rowan-Robinson, A.Efstathiou*, Mon. Notic. Roy. Astr. Soc., **263**, 675, 1993.